Catalysis Science & Technology

Zirconium and Hafnium Polyhedral Oligosilsesquioxane Complexes - Green Homogeneous Catalysts in the Formation of Bio-Derived Ethers via a MPV/Etherification Reaction Cascade

Journal:	*Catalysis Science & Technology*
Manuscript ID	CY-COM-09-2020-001864.R2
Article Type:	Communication
Date Submitted by the Author:	22-Oct-2020

Complete List of Authors:	Krempner, Clemens; Texas Tech University, Department of Chemistry and Biochemistry Garg, Shipra; Texas Tech University Unruh, Daniel; Texas Tech University, Chemistry and Biochemistry

ARTICLE

Zirconium and Hafnium Polyhedral Oligosilsesquioxane Complexes – Green Homogeneous Catalysts in the Formation of Bio-Derived Ethers via a MPV/Etherification Reaction Cascade

Received 00th January 20xx,
Accepted 00th January 20xx

DOI: 10.1039/x0xx00000x

Shipra Garg, Daniel K. Unruh and Clemens Krempner *

The polyhedral oligosilsesquioxane complexes {[(isobutyl)$_7$Si$_7$O$_{12}$]ZrOPr^i·(HOPr^i)}$_2$ (**I**), {[(cyclohexyl)$_7$Si$_7$O$_{12}$]ZrOPr^i·(HOPr^i)}$_2$ (**II**), {[(isobutyl)$_7$Si$_7$O$_{12}$]HfOPr^i·(HOPr^i)}$_2$ (**III**) and {[(cyclohexyl)$_7$Si$_7$O$_{12}$]HfOPr^i·(HOPr^i)}$_2$ (**IV**), were synthesized in good yields from reactions of M(OPr^i)$_4$ (M = Zr, Hf) with R-POSS(OH)$_3$ (R = isobutyl, cyclohexyl), resp. **I**-**IV** were characterized by ^{1}H, ^{13}C and ^{29}Si NMR spectroscopy and their dimeric solid-state structures confirmed by X-ray analysis. **I**-**IV** catalyze the reductive etherification of 2-hydrox- and 4-hydroxy, 2-methoxy and 4-methoxybenzaldehyde and vanillin to their respective isopropyl ethers in isopropanol as "green" solvent and reagent. **I**-**IV** are durable and robust homogeneous catalysts operating at temperatures of 100-160°C for days witout significant loss of catalytic activity. Likewise, **I**-**IV** selectively catalyze the conversion of 5-hydroxymethylfurfural (HMF) to 2,5-bis(isopropoxymethyl)furane (BPMF), a potential high performance fuel additive. Similar results were achieved by using a combination of M(OPr^i)$_4$ and ligand R-POSS(OH)$_3$ as catalyst system demonstrating the potential of this "in situ" approach for applications in biomass transformations. A tentative reaction mechanism for the reductive etherification of aldehydes catalysed by **I**-**IV** is proposed.

Introduction

The chemical conversion of cellulosic biomass into liquid fuel, is a subject of current interest from both the industrial as well as the academic perspective [1]. Particularly alkyl ether have become intensively investigated in the last few years owing to their potential application as high performance fuel additives [2]. One of the most promising synthetic strategies to alkyl ethers involves the reductive etherification of biomass derived aldehydes via Meerwein-Ponndorf-Verley (MPV) reaction followed by acid catalysed etherification (Scheme 1) [3].

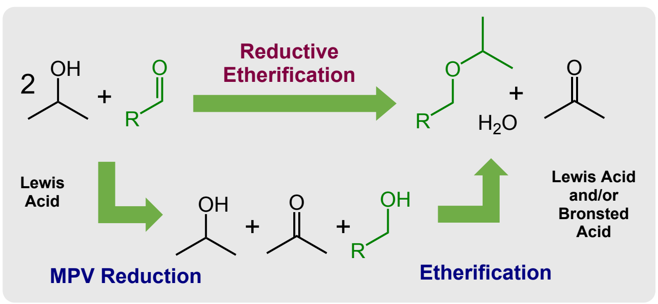

Scheme 1. Ether formation from aldehydes via a reductive etherification cascade.

[a] *Department of Chemistry and Biochemistry, Texas Tech University, Memorial Dr. & Boston, Lubbock, TX, 79409, USA. Fax: 806-742-1289; Tel: 806-834-3507; E-mail: clemens.krempner@ttu.edu*
† Footnotes relating to the title and/or authors should appear here.
Electronic Supplementary Information (ESI) available: [details of any supplementary information available should be included here]. See DOI: 10.1039/x0xx00000x

This process is operationally simple and environmentally friendly as it utilizes "green" isopropanol as an inexpensive, safe and non-toxic solvent and hydrogen transfer reagent in combination with cheap and abundant acid catalysts. The MPV reduction [4], the first step in the cascade, proceeds via Lewis acid catalysed hydrogen transfer usually from a secondary alcohol to the carbonyl substrate with high selectivity, following an outer sphere mechanism [5], while the etherification proceeds with elimination of water and can be catalysed by both, Brønsted or Lewis acid catalysts. Indeed, some heterogeneous tin, zirconium and hafnium zeolite and oxide based catalysts have been reported to convert 5-hydroxymethylfurfural (HMF), a platform chemical for biofuels, biochemical and biopolymers [6], to 2,5-bis(isopropoxy-methyl)furan (BPMF) [7] via reductive etherification. In contrast, homogeneous catalysts capable of converting HMF to BPMF with high selectivity and yields have not yet been reported [8].

Early transition metal "polyhedral" oligosilsesquioxane (POSS) complexes [9] of tripodal coordination geometry are a largely overlooked class of robust and durable metal complexes that have shown some potential as homogeneous catalysts in alkene epoxidations [10] and polymerizations [11]. The electron-withdrawing property of the POSS ligand combined with its steric profile gives rise to well-defined metal complexes that possess relatively high Lewis acidity while maintaining good chemical resistance. Herein we will introduce zirconium and hafnium POSS complexes as a new class of highly efficient and thermally remarkably robust homogeneous catalysts for selected biomass transformations as demonstrated for the reductive etherification of HMF to biofuel additive BMPF.

Results and Discussion

The synthesis of the targeted zirconium and hafnium POSS complexes **I-IV** is illustrated in Scheme 2. Reaction of the commercially available trisilanols R-POSS(OH)$_3$ (R = isobutyl or cyclohexyl) with Zr(OPr^i)$_4$ and Hf(OPr^i)$_4$, respectively, gave after removal of solvent and precipitation or recrystallization from isopropanol (IPA) compounds **I-IV** in 58-66% yield. **I-IV** are thermally stable crystalline materials, which show good solubility in toluene, hexanes, benzene, dichloromethane, diethyl ether and THF but are sparingly soluble in alcohols and DMSO. In addition to be characterized by ^{1}H, ^{13}C and ^{29}Si NMR spectroscopy and combustion analysis, the solid state structures of **I-IV** were determined by X-ray analysis. The results are exemplary shown for **I** and **III** (Figure 1); selected bond lengths and angles for **I-IV** are listed in table 1.

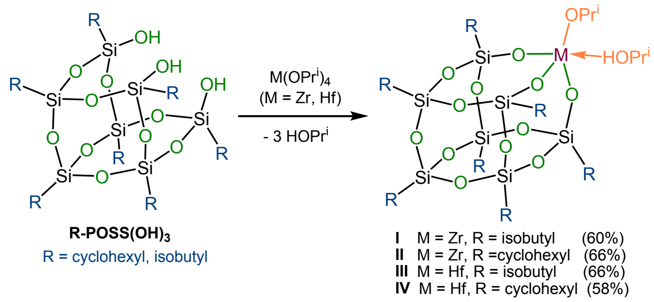

Scheme 2. Synthesis of **I-IV**.

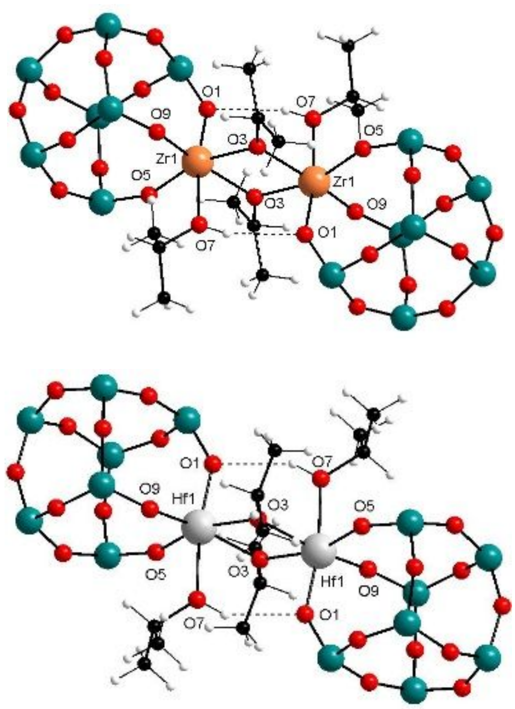

Figure 1. Solid-state structures of **I** (top) and **III** (bottom); isobutyl substituents at silicon are omitted for clarity (blue = silicon, red = oxygen).

In the solid state, all compounds are isostructural dimers with distorted octahedral coordination environments for zirconium and hafnium, respectively, and two isopropanol molecules each coordinating to one of the metal centres, similar to what is seen for other titanium and zirconium analogues [12]. The dimers are held together via bridging isopropoxide groups, and hydrogen bond interaction between the OH group of the coordinating isopropanol and an oxygen from one of the metal binding siloxy groups [O1…O7H, 2.99 to 3.12 Å]. There are three types of metal oxygen bonds that result from this structural arrangement; bridging M-O bonds [M1-O3 2.14-2.18 Å], M-O bonds of the coordinating isopropanol [M1-O7 2.26-2.30 Å], and M-O bonds from the supporting POSS ligand [M1-O1/O5/O9 1.97-2.02 Å]. As expected, the M1-O7 distances are significantly longer than those of the bridging M1-O3 and POSS related M-O distances, suggesting relatively weak isopropanol to metal coordination.

Table 1. Selected bond lengths [Å] and angles [°] of **I-IV**.

-	**I** (M = Zr)	**II** (M = Zr)	**III** (M = Hf)	**IV** (M = Hf)
M1-O1	2.015(3)	1.997(1)	1.993(5)	1.995(2)
M1-O3	2.177(3)	2.156(1)	2.136(5)	2.146(2)
M1-O5	1.982(3)	1.988(1)	1.967(5)	1.984(2)
M1-O7	2.304(3)	2.303(2)	2.257(5)	2.274(2)
M1-O9	1.966(3)	1.987(1)	1.973(5)	1.982(2)
O1-M1-O7	164.8(1)	170.4(1)	167.9(2)	170.3(1)
Si-O(M1)^a	1.611(3)	1.612(2)	1.606(5)	1.612(2)

^{a} average values.

With the POSS complexes **I-IV** in hand, we investigated their catalytic performance in the reductive etherification of various benzaldehydes along with their precursors Zr(OPr^i)$_4$ and Hf(OPr^i)$_4$. Initial screening experiments at 25°C-70°C did not show any substrate conversion. Therefore, the experiments were carried out in closed reaction vessels at temperatures ranging from 100°C to 150°C with catalyst loadings of 1 mol%. Isopropanol (IPA) served as solvent and hydrogen transfer reagent and was used as received ("wet"). Conversions and product yields were determined by ^{1}H NMR spectroscopy using CDCl$_3$ as a solvent and 1,3,5-trimethylbenzene as internal standard. The catalytic experiments were triplicated and conversions and product yields were given as average values.

The moisture sensitive precursor Zr(OPr^i)$_4$ and Hf(OPr^i)$_4$ were found to be surprisingly active in selectively reducing benzaldehyde to benzyl alcohol (**1**) in "wet" isopropanol (IPA) with yields of 57% and 80%, respectively, after 24 hours at 100°C (Figure 2). Employing the new POSS complexes **I-IV**, reproducibly allowed for higher yields with catalysts **I** and **III** each producing 91% of **1**. At 150°C no differences in performance were noted between **I-IV**, Zr(OPr^i)$_4$ and Hf(OPr^i)$_4$; all quantitatively reduced benzaldehyde to **1** (Table S1), but did not form benzyl isopropyl ether.

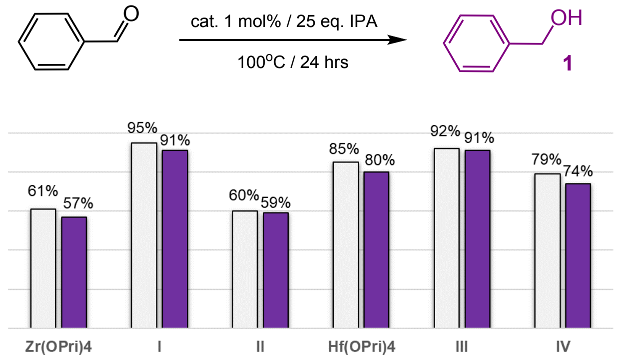

Figure 2. MPV reduction of benzaldehyde to benzyl alcohol 1; conversion (grey bar), yields of alcohol **1** (purple bar).

Next, the reduction of the more electron rich 4-methoxybenzaldehyde was investigated (Figure 3). Similar to what was seen in the previous case, all zirconium and hafnium based catalysts reduced 4-methoxybenzaldehyde to 4-methoxybenzyl alcohol (**2**) in good to excellent yields after 24 hours at 100°C. $Hf(OPr^i)_4$ and **I** showed the best catalyst performances generating 94% of alcohol **2**, respectively.

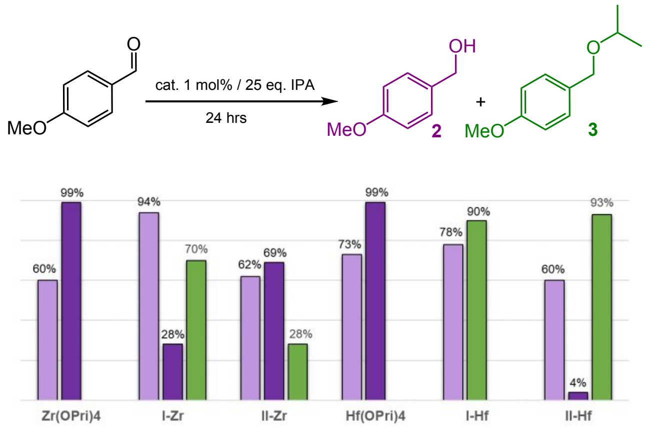

Figure 3. Reductive etherification of 4-methoxybenzaldehyde; yields of alcohol **2** at 100°C (light purple bar); yields of alcohol **2** (dark purple bar), ether **3** (green bar) at 150°C.

Notably, increasing the temperatures from 100 to 150°C not only improved conversions but also changed the selectivity markedly in favour of the targeted 4-methoxybenzyl isopropyl ether (**3**). While $Hf(OPr^i)_4$ and $Zr(OPr^i)_4$ quantitatively converted 4-methoxybenzaldehyde to alcohol **2** only, the hafnium complexes **III** and **IV** selectively produced ether **3** in yields of 90% and 93%, respectively.

2-Methoxybenzaldehyde was converted much faster and with better selectivity to the respective alcohol at 100°C than 4-methoxybenzaldehyde regardless of the catalyst used (Figure 4 and Tables S3-S4). In fact, isobutyl substituted POSS complex **I**, $Zr(OPr^i)_4$ and $Hf(OPr^i)_4$ quantitatively generated 2-methoxybenzyl alcohol **4** in only 3 hours at 100°C. The cyclohexyl substituted complexes **II** and **IV** were slightly less active presumably due to their poor solubility in IPA at 100°C. However, complex **III** proved to be the most active and selective catalyst. **III** not only quantitatively produced alcohol **4** in 1 hour, it also converted alcohol **4** into ether **5** upon increasing the temperature to 150°C. In fact, **III** generated after 24 hours 57% of **5** along with 39% of alcohol **4**. After 48 hours, 82% of **5** and 16% of **4** were formed (Figure 4).

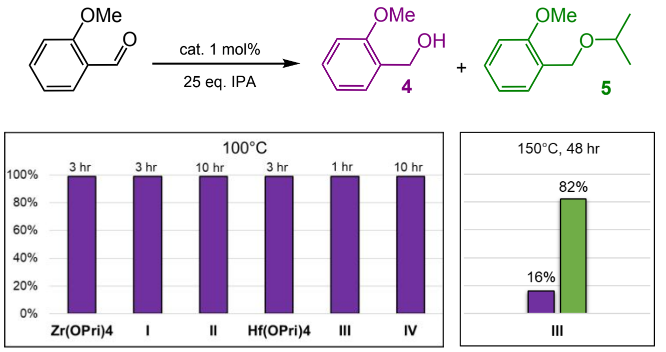

Figure 4. Reductive etherification of 2-methoxybenzaldehyde; graph left) yields of alcohol **4** (purple bar) at various times; graph right) yields of alcohol **4** (purple bar) and ether **5** (green bar) after 48 hours.

Given the structural similarities of **I-IV** (vide supra), it remains unclear why only **III** generates significant amounts of ether **5**. It is known that chelating substrates often cause metal catalyzed reactions to be sluggish because of the inherent strength of the resulting product-metal bonds, typically the limiting factor in product liberation from the metal catalyst. Therefore, even subtle changes of the steric profile (isobutyl versus cyclohexyl substituents) and the identity of the metal (zirconium or hafnium) may account for the differences in product selectivity. Encouraged by the ability to selectively catalyse the formation of ethers, the more challenging substrates 2-hydroxy- and 4-hydroxybenzaldehyde were investigated (Figures 5 and 6). To our surprise, complexes **I-IV** smoothly catalysed the formation of the corresponding isopropyl ethers **7** and **9**, respectively, which were obtained in good to excellent yields after 24 hours. 2-hydroxybenzaldehyde was found to convert to **9** faster and at slightly lower temperatures (120°C) than 4-hydroxybenzaldehyde, which required 125°C to be converted to ether **7** in acceptable yields. Notably, also the precursor $Zr(OPr^i)_4$ and $Hf(OPr^i)_4$ catalysed the formation of the ethers **7** and **9**, respectively, from their respective aldehydes with similar yields but somewhat lower selectivity.

Having had success in selectively producing the hydroxy ethers **7** and **9**, vanillin (4-hydroxy-3-methoxybenzaldehyde), one of the most widely used aroma chemicals and fragrances that can be produced from biomass-derived lignin, was examined (Figure 7). Astonishingly, all zirconium and hafnium catalysts converted vanillin into isopropyl ether **10** with high selectivity and in yields ranging from 68%-91%, even though higher temperatures (150°C) were required relative to the reductive etherification of 2- and 4-hydroxybenzaldehyde. Of all catalysts used, **IV** proved to be the most active system as 91% of ether **10** were formed after 24 hours at 150°C. The catalyst performance of **IV** is similar to that of Rode's dual heterogeneous catalyst, which is composed of $ZrO(OH)_2$ and Zr-Montmorillonite, and gave **10** in 80% yield after 8 hours at 100°C [7c].

Unfortunately, efforts to reduce the phenolic aldehydes 3,4-dihydroxybenzaldehyde, and 4-hydroxy-3,5-methoxybenzaldehyde (syringe aldehyde) failed, after 2 days at 150°C, no conversion was noted. We attribute the inability of these multi-functionalized aldehydes to undergo reduction to their metal chelating properties, resulting in deactivation of the catalyst.

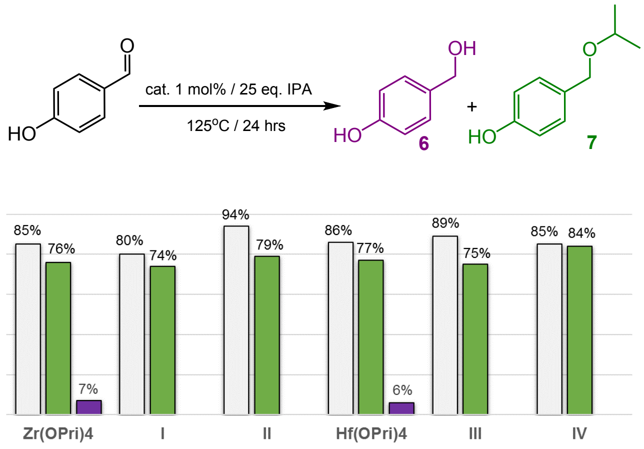

Figure 5. Reductive etherification of 4-hydroxybenzaldehyde. Conversions (grey bar); yields of alcohol **6** (purple bar); yields of ether **7** (green bar).

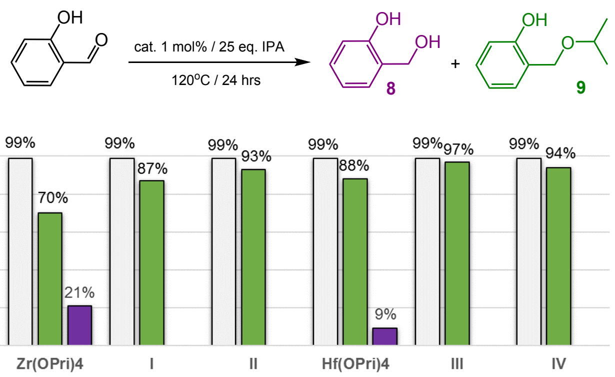

Figure 6. Reductive etherification of 4-hydroxybenzaldehyde. Conversions (grey bar); yields of alcohol **8** (purple bar); yields of ether **9** (green bar).

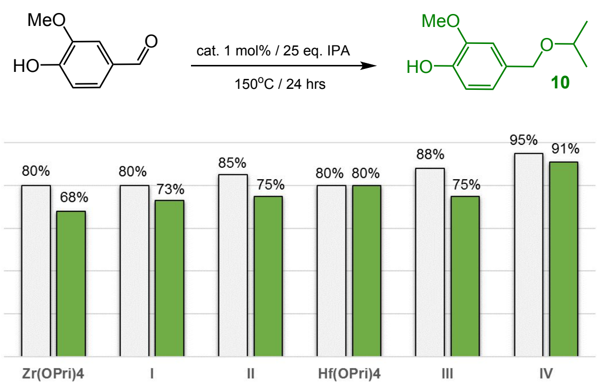

Figure 7. Reductive etherification of vanillin. Conversions (grey bar); yields of ether **10** (green bar).

In comparing the results described above we noticed that $Zr(OPr^i)_4$ and $Hf(OPr^i)_4$ were fairly active in catalysing the formation of the hydroxy ethers **7**, **9** and **10**, but did not catalyse the formation of the methoxy ethers **3** and **5**. Moreover, 2- and 4-hydroxybenzaldehyde were converted faster and with better selectivity to the corresponding ethers than 2- and 4-methoxybenzaldehyde regardless of the catalyst used. At first glance, this appeared to be counter intuitive as according to the Hammett sigma constants, OH groups are somewhat stronger electron donors than methoxy groups. This results in lower carbonyl activities for 2- and 4-hydroxybenzaldehyde, and consequently would lead to lower rates of reduction.

To gain more insights, the kinetic profiles of the reductive etherification for all five benzaldehydes were obtained at 100°C with 1 mol% of **III** as the catalyst; the results are shown in Figures 8 and 9. Consistent with our expectation based on Hammett constants, the rate of conversion was found to be in the order C_6H_5CHO (82%; 16 hours) > 4-MeO-C_6H_4CHO (60%; 16 hours) > 4-HO-C_6H_4CHO (43%; 16 hours).

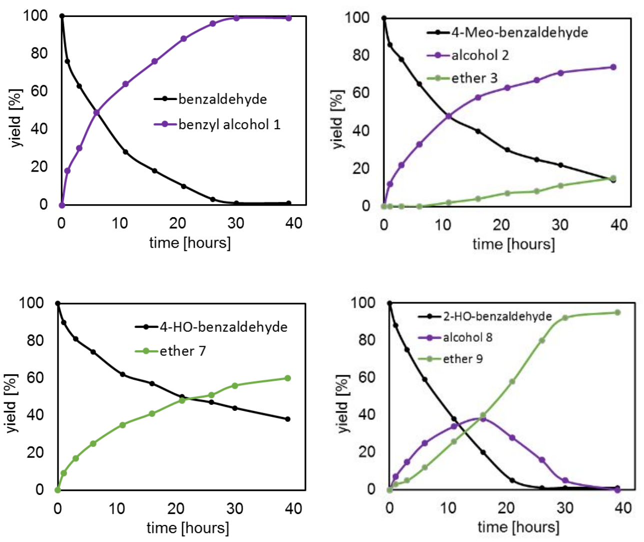

Figure 8. Kinetic profiles of the reductive etherification of (a) benzaldehyde, (b) 4-MeO-benzaldehyde, (c) 4-HO-benzaldehyde, and (d) 2-HO-benzaldehyde. Reaction conditions: 100°C, cat. **III** (1 mol%), 25 eq. isopropanol (IPA).

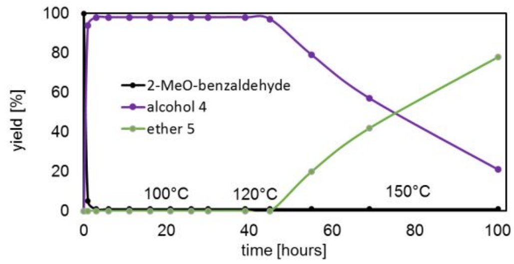

Figure 9. Kinetic profiles of the reductive etherification of 2-MeO-benzaldehyde as a function of temperature. Reaction conditions: 100°C (0-39 hours), 120°C (39-45 hours), 100°C (45-99 hours); cat. **III** (1 mol%), 25 eq. isopropanol (IPA).

The catalytic behaviour of **III** in the reductive etherification of 2-methoxybenzaldehyde (Figure 9) warrants an additional comment. After having catalysed the quantitative formation of alcohol **4** in less than an hour, and being further heated at 100°C for 39 hours and at 120°C for additional 6 hours, **III** still preserves its catalytic activity. In fact, upon subsequently increasing the temperature to 150°C, alcohol **4** slowly converts to ether **5**, demonstrating the catalysts long-term durability and robustness at high temperatures over extensive periods of time and in the presence of water.

We noticed that benzaldehyde and 2-methoxybenzaldehyde exclusively converted to their respective alcohols, and only 4-methoxybenzaldehyde produced small quantities of ether after 30 hours at 100°C. Therefore, it is reasonable to assume that the slow step of the reductive etherification for these substrates is the metal catalysed alcohol etherification. Ether formation, most likely proceeds via a metal stabilized intermediate of carbo-cationic character generated from proton migration of one of the coordinating IPA molecules (Scheme 3). Additional stabilization arises from the electron-donating 4-MeO group, enabling an intramolecular nucleophilic attack of isopropoxide to form the ether bond.

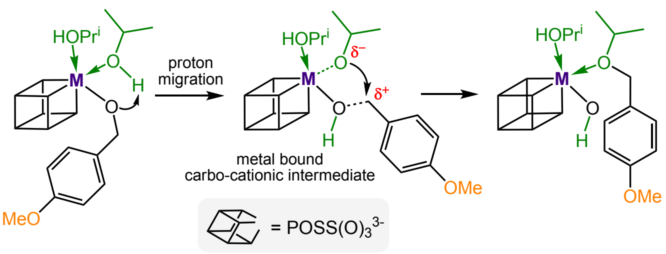

Scheme 3. Proposed ether formation via metal bound carbo-cationic intermediate.

The active involvement of such intermediate appears to be consistent with the observation that at 150°C, the methoxy alcohols **2** and **4** convert to their respective ethers but not benzyl alcohol **1**, i.e. the cationic benzyl intermediate is markedly less stable than the 2- and 4-methoxy substituted counterparts. One of the key factors that enables rapid and selective ether formation seem to be the Lewis acidity of the catalyst system. This is supported by the observation that **I-IV** catalyse the etherification of the methoxy alcohols **2** and **4** but not $Zr(OPr^i)_4$ and $Hf(OPr^i)_4$, i.e. **I-IV** are stronger Lewis acids than their precursors because of the stronger electron-withdrawing properties of the POSS ligand versus an aliphatic alkoxide ligand [13].

By contrast, the precursors $Zr(OPr^i)_4$ and $Hf(OPr^i)_4$ not only catalyse the reductive etherification of 2- and 4-hydroxybenzaldehyde and vanillin (Figures 5-7), their activity is surprisingly similar to those of **I-IV**. In addition, the kinetic results for catalyst **III** (Figures 8 and 9) further confirm that 2- and 4-hydroxybenzaldehyde were converted much faster to the respective ethers than 2- and 4-methoxybenzaldehyde. That 4- and 2-hydroxy groups are somewhat better electron donors than their 4- and 2-methoxy counterparts, and therefore will better stabilize the carbo-cationic intermediate involved in ether formation (Scheme 3) does not seem to account for these drastic differences in rate. Instead, we propose an alternative mechanism that involves the formation of ortho- or para-quinone methide intermediates [14], which are formed via proton migration of the phenolic proton followed by cleavage of the benzylic C-O bond (Scheme 4). These reactive Michael acceptors, which have been generated from various organic precursors and used extensively in synthetic organic chemistry [15], can be described as benzylic cations that are strongly stabilized by the resonance electron donating 4-O$^-$ or 2-O$^-$ substituents [16]. As a result, they are more stable than the cationic methoxybenzyl intermediates involved in the formation of the methoxy ethers **3** and **5**, nonetheless, can readily be attacked by the external nucleophile isopropanol (present in excess) to form the corresponding hydroxy ethers **7**, **9** and **10**, respectively.

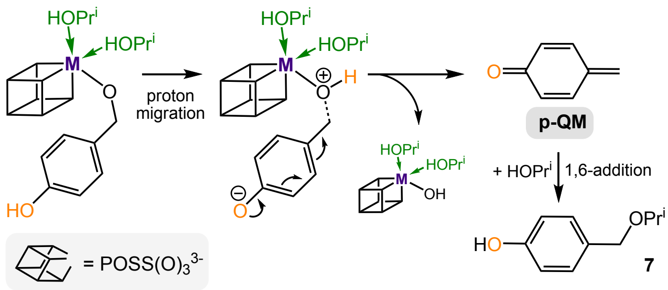

Scheme 4. Proposed alternative formation of hydoxy ether **7** via a metal stabilized para-quinone methide intermediate (p-QM = para-quinone methide).

We next investigated the reduction of HMF, an important renewable feedstock for various bio-based organic compounds such as 2,5-bis(hydroxymethyl)furan (BHMF) (**11**), furan-dicarboxylic acid, levulinic acid, ethyl levulinate and derivatives thereof. Employing Sn-Beta as the catalyst, Vlachos and co-worker reported the formation of BPMF (**12**) from HMF with 87% selectivity and up to 80% overall yield at 180°C [7b]. Rode et al. disclosed the conversion of HMF to BPMF (**12**) in isopropanol at 150°C with claimed selectivity of up to 95% using the dual catalysts, $ZrO(OH)_2$ and Zr-Montmorillonite [7c]. However, in neither cases have isolated yields been reported.

As the reductive etherification of HMF is a complex chemical transformation that involves the formation of humin polymers [17] and various other synthetic intermediates [7c], we were pleased to see that the simple precursor $Zr(OPr^i)_4$ and $Hf(OPr^i)_4$ selectively generated BHMF (**11**) in good yields of 58% and 59%, resp., in only 4 hours at 150°C (Figure 10).

In contrast, catalysts **I-IV** quantitatively converted HMF to primarily humin polymers and the desired BPMF (**12**), albeit the latter in fairly low yields (25-30%). Increasing the reaction time proved to be counter-productive as the yields of **12** further decreased in favour of humin polymers, a common problem in this chemistry [17]. To suppress the formation of humin polymers, a series of experiments was undertaken, where the HMF concentration was gradually decreased by increasing the amounts of isopropanol, from 25 up to 200 eq. using **III** as the catalyst at 150°C. The most relevant results are summarized in Figure 11 (see also Figures S17-S21) and revealed the optimum conditions for this process to be ca. 9-10 hours and 100 eq. of isopropanol. Gratifyingly, after 9 hours, both HMF and undesired BHMF (**11**) were fully consumed, and the reaction mixture only contained ca. 60% BPMF (**12**) and polymer, which greatly facilitated the purification process. Again, increasing the reaction time led to a slight decrease in the yields of **12** due to polymer formation.

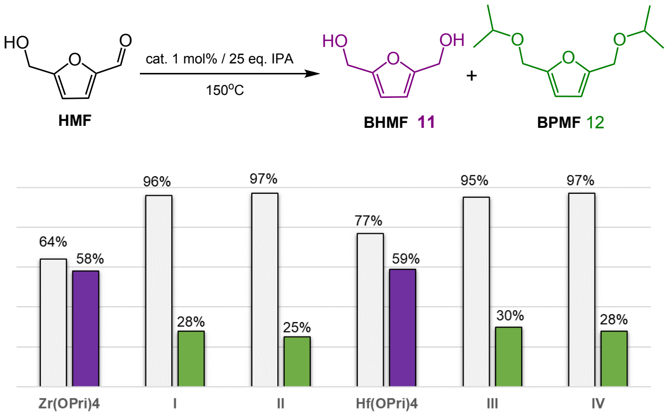

Figure 10. Reductive etherification of 2-hydroxymethylfurfural (HMF). Conversions (grey bar) and product yields (purple bar = **11**; green bar = **12**) after 4 hours.

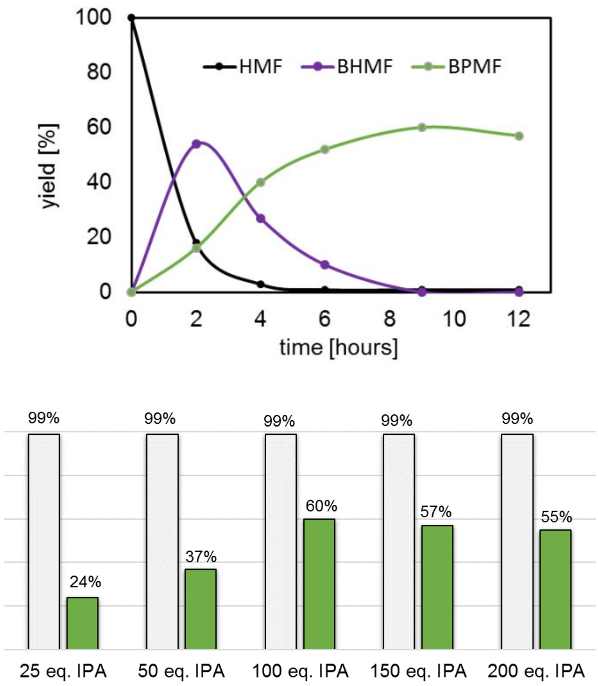

Figure 11. Reductive etherification of HMF as a function of isopropanol (IPA) eq.; cond.: 9 hours; 150°C, cat. **III** (1 mol%); top) Kinetic profile for 100 eq. of IPA; bottom) conversion (grey bar) and yields of BPMF **12** (green bar) for various eq. of IPA.

To demonstrate the practicality of our homogeneous catalyst approach, scale-up syntheses of the ethers **3**, **5**, **7**, **9**, **10** and **12** (1 g substrate) were carried out employing the best performing catalysts, resp. (Scheme 5). All products except **7** could easily be purified by vacuum distillation with isolated yields ranging from to 31-94% [18] without the need of tedious purification by column chromatography.

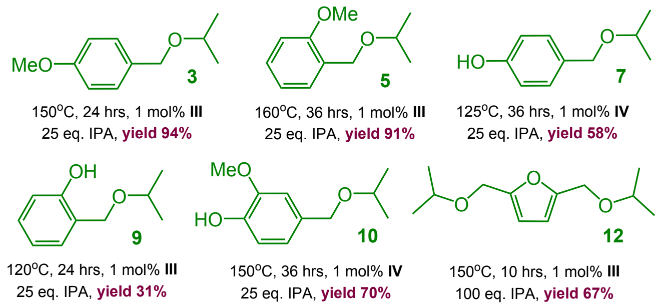

Scheme 5. Gram scale synthesis of **3**, **5**, **7**, **9**, **10** and **12**.

The efficacy and robustness of catalyst **III** in the conversion of HMF to BPMF (**12**), prompted us to test the catalytic activity of $Hf(OPr^i)_4$ (1 mol%) in the presence of ligand Bu^i-POSS$(OH)_3$ (Scheme 6). Gratifyingly, after ca. 10 hours at 150°C (100 eq. IPA) and subsequent purification by vacuum distillation, BPMF could be isolated in 69% yield, similar to what was observed with isolated **III** as the catalyst. Since $Hf(OPr^i)_4$ itself does not produce BPMF (vide supra), catalyst **III** appears to have formed during the course of the reaction. This "in situ" catalyst approach could also be applied to the catalytic formation of the ethers **3**, **5** and **10** with comparable isolated yields but somewhat longer reaction times (see SI).

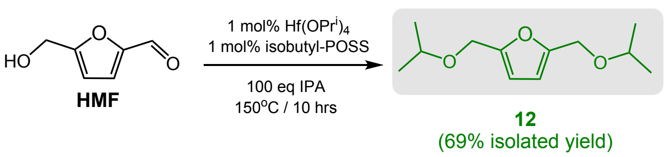

Scheme 6. Synthesis of **10** and **12** employing 1 mol% $Hf(OPr^i)_4$ and 1 mol% Bu^i-POSS$(OH)_3$.

To study the catalysts structure in solution, diffusion experiments for hafnium complex **III** using DOSY-NMR spectroscopy were performed in various solvents at room temperature. The results for THF-D_8 and C_6D_6 clearly suggest **III** to be dimeric in solution, which is consistent with its solid-state structure. In the more polar solvents CD_2Cl_2 and acetone-D_6, however, **III** was found to be monomeric (for more details see SI).

Based on these observations and those discussed above we propose a tentative mechanism, where **III** exist in isopropanol as a hexa-coordinate monomeric complex of type **A** (Scheme 7). For the MPV reduction to occur, complex **A**, which bears two coordinating IPA molecules needs to be in rapid equilibrium with its substrate-metal complex **B** to allow for an intramolecular transfer of hydride from the isopropoxide to the substrate. Complex **C** thus generated converts via replacement of the coordinated acetone product with excess IPA to species **D**. To enable the second step of the overall process, the etherification, an intramolecular proton transfer in **D** from the coordinated IPA to the benzyloxide needs to occur. Complex **E** thus generated subsequently undergoes an intramolecular nucleophilic substitution to furnish the ether bound metal-hydroxide **F**. Liberation of the coordinating ether product from **F** via replacement with excess IPA produces metal hydroxide **G**. Subsequent intramolecular proton transfer from the coordinating IPA to the hydroxide generates complex **G**, which upon replacement of the coordinating water by excess IPA finally converts to catalyst **A**. Note that in case of the 2- and 4-hydroxybenzaldehyde and vanillin as substrates proton migration in species D will occur involving the phenolic proton. This is followed by C-O bond cleavage and formation of ortho- or para-quinone methide intermediates (see also Scheme 4).

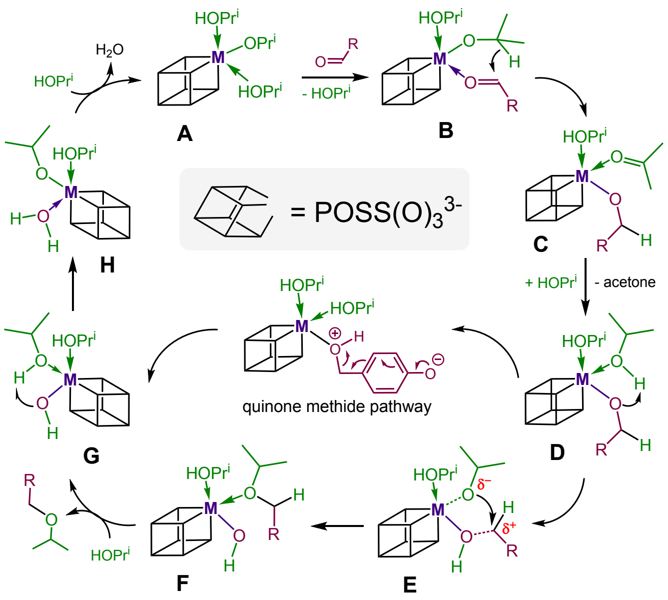

Scheme 7. Proposed reaction mechanism of the reductive etherification of aldehydes.

Conclusions

With the goal of developing durable homogeneous catalysts for selective biomass transformations, we have synthesized the tripodal zirconium and hafnium isopropoxides **I-IV**. In these "corner capped" complexes, zirconium and hafnium are rigidly incorporated into the electron-withdrawing POSS(O)$_3^{3-}$ ligand framework, which provides complexes **I-IV** with sufficient Lewis acidity, high kinetic stability and thermal robustness. In fact, **I-IV** are efficient homogeneous catalysts operating at low loadings and high temperatures in the reductive etherification of electron-rich aromatic aldehydes to produce various isopropyl ethers. Zr(OPr^i)$_4$ and Hf(OPr^i)$_4$ are active catalysts themselves, showing excellent selectivity toward the formation of the alcohols **4**, **6** and **11** but are inactive regarding ether formation. These selectivity differences can be interpreted in terms of their different Lewis acidities. In contrast, **I-IV** and Zr(OPr^i)$_4$/Hf(OPr^i)$_4$ performed with similar activity and selectivity to generate the hydroxyl ethers **7**, **9** and **10**, which we attribute to the involvement of para- and ortho-quinone methide intermediates. Most importantly, **III** proved to be the first homogeneous catalyst capable of selectively converting HMF to bio-fuel additive BPMF (**12**), the latter could be isolated in good yields and purities upon distillation. That similar catalytic performances can be achieved without the need of synthesizing the POSS catalyst, as demonstrated for the selective conversion of HMF to BPMF, highlights the potential of our homogeneous approach for applications in biomass and related transformations.

Conflicts of interest

There are no conflicts to declare.

Acknowledgements

This research was supported by the U.S. Department of Energy, Office of Science, Office of Basic Energy Sciences, Catalysis Science Program, under Award DE-SC0019094. We are grateful to Anthony Cozzolino for calculating the Van der Waals volume of complex **III** and Shiva Moaven for assisting in the DOSY-NMR experiments.

Notes and references

1 a) M. J. Climent, A. Corma and S. Iborra, *Green Chem.* 2014, **16**, 516-547; b) J. C. Serrano-Ruiz and J. A. Dumesic, *Energy Environ. Sci.* 2011, **4**, 83-99; c) D. M. Alonso, J. Q. Bond and J. A. Dumesic, *Green Chem.* 2010, **12**, 1493-1513.

2 a) A. Liu, B. Liu, Y. Wang, R. Ren and Z. Zhang, *Fuel* 2014, **117**, 68-73; b) M. Balakrishnan, E. R. Sacia and A. T. Bell, *Green Chem.* 2012, **14**, 1626-1634; c) M. Musolino, M. J. Gines-Molina, R. Moreno-Tost and Fabio Arico, *ACS Sustainable Chem. Eng.* 2019, **7**, 10221-10226.

3 a) A. Corma and M. Renz, *Angew. Chem. Int. Ed.* 2007, **46**, 298-300; b) A. M. Rasero-Almansa, M. Iglesias, and F. Sanchez, *RSC Advances* 2016, **6**, 106790-106797; c) G. Li, L. Gao, Z. Sheng, Y. Zhan, C. Zhang, J. Ju, Y. Zhang and Y. Tang, *Catal. Sci. Technol.* 2019, **9**, 4055-4065.

4 a) C. Battilocchio, J. M. Hawkins and S. V. Ley, *Org. Lett.* 2013, **15**, 2278-2281; b) B. McNerney, B. Whittlesey, D. B. Cordes and C. Krempner, *Chem. Eur. J.* 2014, **20**, 14959-14964; c) X. Wang, J. Hao, L. Deng, H. Zhao, Q. Liu, N. Li, R. He, K. Zhi and H. Zhou, *RSC Advances* 2020, **10**, 6944-6952; d) A. Corma, M. E. Domine, L. Nemeth and S. Valencia, *J. Am. Chem. Soc.* 2002, **124**, 3194-3195; e) K. Flack, K. Kitagawa, P. Pollet, C. A. Eckert, K. Richman, J. Stringer, W. Dubay and C. L. Liotta, *Org. Process Res. Dev.* 2012, **16**, 1301-1306.

5 a) R. Cohen, C. R. Graves, S. T. Nguyen, J. M. L. Martin and M. A. Ratner, *J. Am. Chem. Soc.* 2004, **126**, 14796-14803; b) O. Eisenstein and R. H. Crabtree, *New J. Chem.* 2013, **37**, 21-27; c) R. S. Assary, L. A. Curtiss and J. A. Dumesic, *ACS Catal.* 2013, **3**, 2694-2704.

6 a) R.-J. van Putten, J. C. van der Waal, E. de Jong, C. B. Rasrendra, H. J. Heeres and J. G. de Vries. *Chem. Rev.* 2013, **113**, 1499-1597; b) S. Chen, R. Wojcieszak, F. Dumeignil, E. Marceau and S. Royer, *Chem. Rev.* 2018, **118**, 11023–11117.

7 a) J. Luo, J. Yu, R. J. Gorte, E. Mahmoud, D. G. Vlachos and M. A. Smith, *Catal. Sci. Technol.* 2014, **4**, 3074–3081; b) J. Jae, E. Mahmoud, R. F. Lobo and D. G. Vlachos, *ChemCatChem* 2014, **6**, 508-513; c) S. Shinde and C. Rode, *ChemSusChem* 2017, **10**, 4090-4101.

8 H. Nguyen, N. Xiao, S. Daniels, N. Marcella, J. Timoshenko, A. Frenkel and D. G. Vlachos, *ACS Catalysis* 2017, **7**, 7363-7370.

9 a) F. J. Feher and T. A. Budzichowski, *Polyhedron* 1995, **14**, 3239-3253; b) D. B. Cordes, P. D. Lickiss and F. Rataboul,

Chem. Rev. 2010, **110**, 2081-2173; c) C. Krempner, *Eur. J. Inorg. Chem.* 2011, **2011**, 1689-1698.

10 a) H. C. L. Abbenhuis, S. Krijnen and R. A. van Santen, *Chem. Comm.* 1997, 331-332; b) T. Maschmeyer, M. C. Klunduk, C. M. Martin, D. S. Shephard, J. M. Thomas and B. F. G. Johnson, *Chem. Comm.* 1997, 1847-1848; c) M. Crocker, R. H. M. Herold and A. G. Orpen, *Chem. Comm.* 1997, 2411-2412; d) F. Carniato, C. Bisio, E. Boccaleri, M. Guidotti, E. Gavrilova and L. Marchese, *Chem. Eur. J.* 2008, **14**, 8098-8101; e) E. H. Aish, M. Crocker and F. T. Ladipo, *J. Catalysis* 2010, **273**, 66-72; f) M. D. Skowronska-Ptasinska, M. L.-W. Vorstenbosch, R. A. van Santen and H. C. L. Abbenhuis, *Angew. Chem., Int. Ed.* 2002, **41**, 637-639; g) L. Zhang, H. C. L. Abbenhuis, G. Gerritsen, N. N. Bhriain, P. C. M. Magusin, B. Mezari, W. Han, R. A. van Santen, Q. Yang and C. Li, *Chem. Eur. J.* 2007, **13**, 1210-1221; h) P. Guillo, M. I. Lipschutz, M. E. Fasulo and T. D. Tilley, *ACS Catalysis* 2017, **7**, 2303-2312.

11 a) F. J. Feher, J. F. Walzer and R. L. Blanski, *J. Am. Chem. Soc.* 1991, **113**, 3618-3619; b) F. J. Feher and R. L. Blanski, *J. Am. Chem. Soc.* 1992, **114**, 5886-5887; c) R. Duchateau, H. C. L. Abbenhuis, R. A. van Santen, A. Meetsma, S. K.-H. Thiele and M. F. H. van Tol, *Organometallics* 1998, *17*, 5663-5673.

12 a) O. Viotti, A. Fischer, G. A. Seisenbaeva and V. G. Kessler, Inorg. *Chem. Comm.* 2010, **13**, 774-777; b) O. Viotti, G. A. Seisenbaeva and V. G. Kessler, *Inorg. Chem.* 2009, **48**, 9063-9065.

13 a) F. J. Feher and T. A. Budzichowski, *J. Organomet. Chem.* 1989, **379**, 33-40; b) R. West and R. H. Baney, *J. Am. Chem. Soc.* 1959, **81**, 6145-6148; c) R. West, R. H. Baney and D. L. Powell, J. Am. Chem. Soc. 1960, **82**, 6269-6272; d) P. T. Wolczanski, *Polyhedron* 1995, **14**, 3335-3362; e) C. Krempner, *Eur. J. Inorg. Chem.* 2011, 1689-1698.

14 a) S. E. Rokita (ed.) Quinone Methides (John Wiley and Sons, 2009); b) E. Dorrestijn, M. Kranenburg, M. V. Ciriano and P. Mulder, *J. Org. Chem.* 1999, **64**, 3012-3018; b) S. J. Gharpure, A. M. Sathiyanarayanan and P. Jonnalagadda, *Tetrahedron Lett.* 2008, **49**, 2974-2978; c) M. M. Toteva, M. Moran, T. L. Amyes and J. P. Richard, *J. Am. Chem. Soc.* 2003, **125**, 8814-8819.

15 a) E. E. Weinert, R. Dondi, S. Colloredo-Melz, K. N. Frankenfield, C. H. Mitchell, M. Freccero and S. E. Rokita, *J. Am. Chem. Soc.* 2006, **128**, 11940-11947; b) R. W. Van de Water and T. R. R. Pettus, *Tetrahedron* 2002, **58**, 5367–5405; c) W.-J. Bai, J. G. David, Z.-G. Feng, M. G. Weaver, K.-L. Wu and R. R. Pettus, *Acc. Chem. Res.* 2014, **47**, 3655−3664.

16 M. M. Toteva and J. P. Richard, *Adv. Phys. Org. Chem.* 2011, **45**, 39-91.

17 G. Tsilomelekis, M. J. Orella, Z. Lin, Z. Cheng, W. Zheng, V. Nikolakis and D. G. Vlachos. *Green Chem.* 2016, **18**, 1983-93.

18 The low yield of ether **9** after distillation is the result of a thermal fragmentation to the ortho-quinone methide followed by polymerization to undefined products. See also: d) S. B. Cavith, H. R. Sarrafizadeh and P. D. Gardner, *J. Org. Chem.* 1962, **27**, 1211-1216.

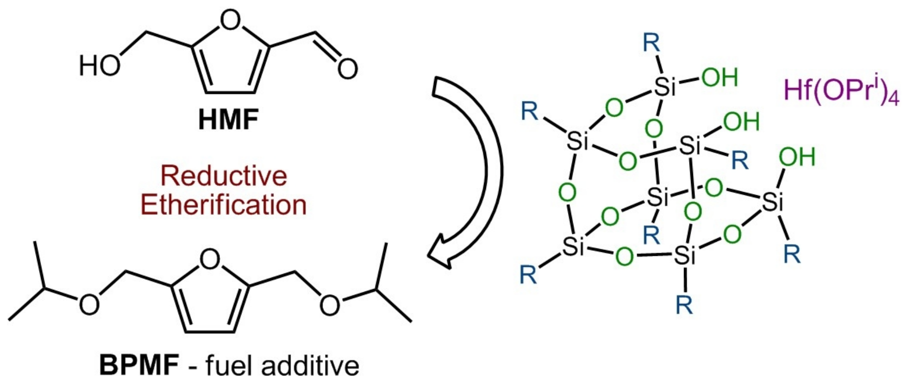

338x190mm (96 x 96 DPI)